Neuropilin-2 regulates airway inflammatory responses to inhaled lipopolysaccharide

Robert M. Immormino,[1] David C. Lauzier,[2] Hideki Nakano,[3] Michelle L. Hernandez,[1,2] Neil E. Alexis,[1,2] Andrew J. Ghio,[4] Stephen L. Tilley,[5] Claire M. Doerschuk,[5] David B. Peden,[1,2] Donald N. Cook,[3]* and Timothy P. Moran[1,2]*

[1]*Center for Environmental Medicine, Asthma and Lung Biology, University of North Carolina, Chapel Hill, North Carolina;* [2]*Department of Pediatrics, University of North Carolina, Chapel Hill, North Carolina;* [3]*Immunity, Inflammation and Disease Laboratory, Division of Intramural Research, National Institute of Environmental Health Sciences, National Institutes of Health, Research Triangle Park, North Carolina;* [4]*National Health and Environmental Effects Research Laboratory, Environmental Protection Agency, Chapel Hill, North Carolina; and* [5]*Department of Medicine, University of North Carolina, Chapel Hill, North Carolina*

Submitted 6 February 2018; accepted in final form 13 April 2018

Immormino RM, Lauzier DC, Nakano H, Hernandez ML, Alexis NE, Ghio AJ, Tilley SL, Doerschuk CM, Peden DB, Cook DN, Moran TP. Neuropilin-2 regulates airway inflammatory responses to inhaled lipopolysaccharide. *Am J Physiol Lung Cell Mol Physiol* 315: L202–L211, 2018. First published April 19, 2018; doi:10.1152/ajplung.00067.2018.—Neuropilins are multifunctional receptors that play important roles in immune regulation. Neuropilin-2 (NRP2) is expressed in the lungs, but whether it regulates airway immune responses is unknown. Here, we report that *Nrp2* is weakly expressed by alveolar macrophages (AMs) in the steady state but is dramatically upregulated following in vivo lipopolysaccharide (LPS) inhalation. Ex vivo treatment of human AMs with LPS also increased *NRP2* mRNA expression and cell-surface display of NRP2 protein. LPS-induced *Nrp2* expression in AMs was dependent upon the myeloid differentiation primary response 88 signaling pathway and the transcription factor NF-κB. In addition to upregulating display of NRP2 on the cell membrane, inhaled LPS also triggered AMs to release soluble NRP2 into the airways. Finally, myeloid-specific ablation of NRP2 resulted in increased expression of the chemokine (C-C motif) ligand 2 (*Ccl2*) in the lungs and prolonged leukocyte infiltration in the airways following LPS inhalation. These findings suggest that NRP2 expression by AMs regulates LPS-induced inflammatory cell recruitment to the airways and reveal a novel role for NRP2 during innate immune responses in the lungs.

airway inflammation; alveolar macrophage; innate immunity; lipopolysaccharide; neuropilin-2

INTRODUCTION

The respiratory tract is constantly exposed to airborne microbes and their products. Recognition of pathogen-associated molecular patterns (PAMPs) by innate immune receptors, such as toll-like receptors (TLRs), is critical for the rapid identification and clearance of inhaled pathogens (22). However, excessive or inappropriate activation of innate immune cells by PAMPs can result in tissue damage and lung injury (27). Therefore, innate immune responses must be tightly regulated to maintain lung homeostasis. Indeed, defects in innate immune regulation are thought to contribute to the development of inflammatory lung diseases, including acute respiratory distress syndrome (19), asthma (20), and chronic obstructive pulmonary disease (4). Identifying the key cellular and molecular mechanisms that regulate innate immune responses in the lungs may lead to new therapies for immune-mediated lung diseases.

Neuropilins are a family of pleiotropic receptors that have important functional roles in the cardiovascular, nervous, and immune systems (18). The two family members, neuropilin-1 (NRP1) and neuropilin-2 (NRP2), are type I transmembrane proteins that share 44% sequence homology (6). Neuropilins also have soluble forms created by alternative splicing (40) or by ectodomain shedding of the transmembrane proteins (45, 47). As coreceptors for secreted class III semaphorins and vascular endothelial growth factor (VEGF) family members, neuropilins are involved with a variety of physiological processes, including neuronal migration, angiogenesis, and cell growth (18). Neuropilins also have essential roles in regulating adaptive and innate immune responses (39). Although the importance of NRP1 in immunity has been well described (25), much less is known about the immunological function of NRP2. NRP2 is expressed by several different immune cells, including thymocytes (31), macrophages (23), and dendritic cells (DCs) (8), and may be involved in directing migration of these cell types (9, 31). NRP2 is also one of only a few proteins that undergo polysialylation in mammals, which can impact immune cell signaling and migration (35). NRP2 was recently reported to be expressed by human lung macrophages (2), but its role in airway immune responses is unknown. Here, we report that *Nrp2* expression in murine alveolar macrophages (AMs) is low under steady-state conditions but is dramatically increased following LPS inhalation through a myeloid differentiation primary response 88 (MyD88)- and NF-κB-dependent mechanism. Ex vivo stimulation of human AMs with LPS also significantly upregulated *NRP2* expression. In addition to increasing cell surface display of NRP2, inhaled LPS also triggered AMs to release soluble NRP2 (sNRP2) into the

* D. N. Cook and T. P. Moran contributed equally to this work.

Address for reprint requests and other correspondence: T. P. Moran, 125 Mason Farm Rd., CB# 7248, Univ. of North Carolina, Chapel Hill, NC 27599 (e-mail: tmoran@email.unc.edu).

airways. Finally, we found that myeloid-specific ablation of NRP2 results in prolonged accumulation of airway monocytes/macrophages and neutrophils following LPS inhalation, which was associated with increased chemokine (C-C motif) ligand 2 (*Ccl2*) expression in the lungs. Taken together, these findings suggest that NRP2 expression by AMs is necessary for suppressing inflammatory responses to inhaled LPS.

MATERIALS AND METHODS

Mice. C57BL/6J, *Nrp2*^{gfp} (*Nrp2*$^{tm1.2Mom}$/MomJ), and LysMcre (B6.129P2-*Lyz2*$^{tm1(cre)Ifo}$/J) mice were obtained from Jackson Laboratories (Bar Harbor, ME). *Nrp2*$^{fl/fl}$ (*Nrp2*$^{tm1.1Mom}$/MomJ) mice were kindly provided by Tracy Tran (Rutgers University). *Myd88*$^{-/-}$ and *Trif*$^{-/-}$ mice were provided by Claire Doerschuk. Female and male mice were housed in specific pathogen-free conditions and used between 6 and 12 wk of age at a weight of 20–25 g. All animal experiments were approved by the Institutional Animal Care and Use Committee at the University of North Carolina at Chapel Hill.

Flow cytometric analysis of murine lung leukocyte populations. Murine lung leukocytes were isolated and analyzed by flow cytometry as previously described (33, 36). Briefly, lungs were harvested from untreated mice or at 16 h after airway instillation of 100 ng lipopolysaccharide (LPS) from *Escherichia coli* O111:B4 (Sigma, St. Louis, MO) or phosphate-buffered saline (PBS). Harvested lungs were minced and digested with Liberase TM (100 μg/ml; Roche, Indianapolis, IN), collagenase XI (250 μg/ml), hyaluronidase 1a (1 mg/ml), and DNase I (200 μg/ml; Sigma) for 1 h at 37°C. The digested tissue was passed through a 70-μm nylon strainer to obtain a single cell suspension. Red blood cells were lysed with 0.15 M ammonium chloride and 1 mM potassium bicarbonate. In some experiments, lung macrophages and DCs were enriched by discontinuous phase-density centrifugation with 16% Nycodenz (Accurate Chemical & Scientific, Westbury, NY) before antibody staining. For antibody staining of surface antigens, cells were incubated with antimouse CD16/CD32 (2.4G2) for 5 min to block Fc receptors, followed by incubation with fluorochrome- or biotin-conjugated antibodies against murine CD3ε (145-2C11), CD11b (M1/70), CD11c (N418), CD19 (6D5), CD88 (20/70), CD103 (M290), Ly-6C (AL-21), Ly-6G (1A8), I-A/E (M5/114.15.2; BioLegend, San Diego, CA); or Siglec-F (E50-2440; BD Biosciences, San Jose, CA) for 30 min on ice. Staining with biotinylated antibodies was followed by incubation with fluorochrome-conjugated streptavidin for 20 min on ice. Cells were also concurrently stained with Zombie Aqua (BioLegend) for live cell/dead cell discrimination. Flow cytometry data were acquired with a four-laser LSRII (BD Biosciences) and analyzed using FlowJo (Treestar, Ashland, OR) software. Only single cells were analyzed. Lung macrophage and DC subpopulations were identified as follows: AMs (CD45$^+$ CD11c^{hi}Siglec-F^{hi}), interstitial macrophages (IMs; CD45$^+$CD88^{hi} CD11b^{hi}I-A/E^{hi}Ly-6C^{lo}), CD11b$^+$ conventional DCs (CD45$^+$Siglec-F^{lo}CD11c^{hi}I-A/E^{hi}Ly-6C^{lo}CD11b^{hi}CD103^{lo}), and CD103$^+$ conventional DCs (CD45$^+$Siglec-F^{lo}CD11c^{hi}I-A/E^{hi}Ly-6C^{lo}CD11b^{lo}CD103^{hi}).

For analysis of surface NRP2 expression, murine AMs were isolated by bronchoalveolar lavage (BAL) as previously described (51). AMs were incubated with anti-mouse CD16/CD32 to block Fc receptors and then incubated with anti-NRP2 polyclonal goat IgG (AF-567; R&D Systems, Minneapolis, MN) or control goat IgG for 30 min. AMs were secondarily stained with Alexa Fluor 647-conjugated anti-goat antigen-binding fragment (Jackson ImmunoResearch, West Grove, PA) for 20 min before flow cytometry analysis.

Isolation and ex vivo treatment of murine AMs. Murine AMs were isolated by BAL as previously described (51) and resuspended in complete RPMI-10 medium [RPMI-1640, 10% fetal bovine serum (Gemini, West Sacramento, CA), penicillin-streptomycin, and 50 ng/ml β-mercaptoethanol]. AMs were seeded into 96-well plates at 10^5 cells/well and treated with LPS (100 ng/ml) or PBS diluent. In some experiments, AMs were pretreated with 10 μg/ml ammonium pyrrolidinedithiocarbamate (PDTC; Sigma), 1 μg/ml BMS-345541 (Sigma), or dimethyl sulfoxide (DMSO) for 1 h before stimulation with LPS.

Isolation and ex vivo treatment of human AMs. Human AMs were recovered from BAL fluid samples obtained from healthy, nonsmoking volunteers, age 18 to 40 yr, under an approved protocol at the University of North Carolina at Chapel Hill. BAL samples contained >90% macrophages as determined by Quick-Diff staining. BAL cells were cultured in 24-well plates for 1–2 h at 37°C to allow adherence of macrophages. After removal of nonadherent cells, adherent macrophages were treated with either 100 ng/ml LPS (Sigma) or PBS diluent and cultured in complete RPMI-10 medium. Cells were harvested at 6 h for RNA isolation or at 24 h for confocal microscopy and flow cytometry analysis. For flow cytometric studies, PBS- or LPS-treated macrophages were first incubated with mouse IgG to block Fc receptors and then stained with fluorescent-conjugated antibodies to CD11c (Bu15), HLA-DR (L243), CD14 (HDC14), and CD45 (HI30; BioLegend). Discrimination of live/dead cells was accomplished by Zombie Aqua (BioLegend) staining. AMs were identified as CD45$^+$CD14^{hi}HLA-DR^{hi} cells. For detection of cell surface NRP2 on human AMs, cells were incubated with goat anti-human NRP2 polyclonal goat IgG (AF-2215; R&D) or control goat IgG antibodies and then secondarily stained with Alexa Fluor 647-conjugated anti-goat Fab fragment (Jackson Immuno Research). For immunofluorescent antibody staining, BAL cells were cultured on poly-L-lysine-coated glass coverslips. After 24 h, the cells were washed with PBS, fixed in 4% paraformaldehyde for 10 min at room temperature, and then permeabilized with PBS containing 0.1% Triton X-100 for 10 min at room temperature. The cells were next blocked in PBS + 0.05% Tween-20 + 1% BSA for 1 h, followed by incubation with primary antibodies overnight at 4°C. After being washed, the cells were incubated with fluorochrome-conjugated secondary antibodies for 1 h at room temperature and counterstained with DRAQ5 (BioLegend). The coverslips were mounted on microscope slides and examined using a Leica SP5 confocal microscope.

Immunoblot analysis. Murine AMs were lysed in radioimmunoprecipitation assay buffer supplemented with a protease inhibitor cocktail (Roche). Total cell lysates, murine BAL fluid, or cell culture supernatants were mixed with Laemmli sample buffer, heated at 98°C for 10 min, separated by sodium dodecyl sulfate (SDS)-polyacrylamide electrophoresis under reducing conditions, and transferred to a PVDF membrane. After being blocked with 5% milk in Tris-buffered saline-Tween 20 buffer, membranes were incubated with anti-mouse/rat NRP2 monoclonal rabbit IgG D-39-A-5 (Cell Signaling Technology, Danvers, MA) at 1:1,000 dilution, followed by incubation with peroxidase-conjugated secondary antibodies. Immunoblots were analyzed on a ChemiDoc MP Imaging System (Bio-Rad, Hercules, CA).

LPS-induced airway inflammation model. Mice were anesthetized by isofluorane inhalation and given 10 μg of LPS in a total volume of 50 μl by oropharyngeal aspiration. At the indicated time points, whole lung lavage was performed, and cell differentials were determined as previously described (48). Levels of total protein in BAL fluid were determined by bicinchoninic acid analysis. For RNA analysis, lungs were perfused with PBS and flash frozen in liquid nitrogen and stored at −80°C until RNA isolation was performed. For histological studies, lungs were fixed in 10% buffered formalin, sectioned and stained with hematoxylin and eosin, and analyzed by microscopy.

cDNA amplification and analysis. Total RNA was isolated from cells or lung tissue using TRIzol reagent (Life Technologies, Grand Island, NY) and converted to cDNA with oligo deoxythymine and random hexamer primers using murine leukemia virus reverse transcriptase (Life Technologies). Quantitative PCR was performed using PerfeCTa SYBR Green PCR Mastermix (Quantabio, Beverly, MA) and a 7300 Real-Time PCR System (Applied Biosystems, Waltham, MA). KiCqStart SYBR Green Primers (Sigma) specific for murine *Nrp2*, *Il6*, *Ppih*, *Cxcl1*, *Cxcl2*, *Cxcl5*, *Ccl2*, *Actb*, and *Gapdh*, or

human *NRP2* and *ACTB* genes were used for PCR amplification. The efficiency-corrected change in threshold cycle for each gene was determined and normalized to *Gapdh* or *Actb*.

Statistical analysis. Data are expressed as means ± SE. Statistical differences between groups were calculated using a two-tailed Student's *t*-test or Mann-Whitney *U*-test. $P < 0.05$ was considered significant.

RESULTS

LPS inhalation induces Nrp2 expression by murine AMs in vivo. To determine if the *Nrp2* gene is expressed in murine lung macrophages and how it is regulated in these cells, we used heterozygous $Nrp^{gfp/+}$ mice in which green fluorescent protein fluorescence reflects *Nrp2* expression. Using multicolor flow cytometry, we analyzed $Nrp2^{gfp}$ expression by lung macrophages and other leukocyte populations (Fig. 1*A*). Under steady-state conditions, $Nrp2^{gfp}$ was expressed in only 1% of AMs and in 5% of IMs (Fig. 1*B*). $Nrp2^{gfp}$ was also expressed in a small percentage of $CD11b^+$ conventional DCs (cDCs), but not in lung $CD103^+$ cDCs, $CD3^+$ T cells, $CD19^+$ B cells, Ly-$6C^+$ monocytes, Ly-$6G^+$ neutrophils, or Siglec-$F^{hi}CD11c^{lo}$ eosinophils (Fig. 1*B*). $Nrp2^{gfp}$ expression was detected in a small percentage of $CD45^-$ cells, which likely represent bronchial epithelial cells (26) or lymphatic endothelial cells (49). Despite their low level of $Nrp2^{gfp}$ expression at steady state, AMs dramatically increased their expression of $Nrp2^{gfp}$ following LPS inhalation, with 60% of AMs acquiring $Nrp2^{gfp}$ expression by 16-h post-LPS treatment (Fig. 1, *C* and *D*). By contrast, this treatment did not significantly increase $Nrp2^{gfp}$ expression in IMs, $CD11b^+$ DCs, or $CD103^+$ cDCs (Fig. 1*C*). Inhaled LPS also failed to induce $Nrp2^{gfp}$ expression in lung granulocytes, lymphocytes or $CD45^-$ cells (data not shown). To confirm our finding with $Nrp2^{gfp/+}$ mice at the protein level, we used flow cytometry to analyze cell surface display of NRP2 protein on AMs from C57BL/6 mice. Consistent with our $Nrp2^{gfp}$ expression studies, cell surface NRP2 display was low on AMs from PBS-treated C57BL/6 mice but significantly increased on AMs from LPS-treated mice (Fig. 1, *E* and *F*). Thus, inhalational exposure to LPS induces *Nrp2* mRNA expression and cell surface display of NRP2 protein by AMs in vivo.

Ex vivo stimulation of human AM with LPS induces NRP2 expression. Given our findings with murine AMs, we next investigated whether LPS similarly induces *NRP2* expression by human AMs. Human AMs from normal individuals were obtained by BAL and treated ex vivo with LPS or PBS diluent. Confocal microscopy revealed that NRP2 was readily detect-

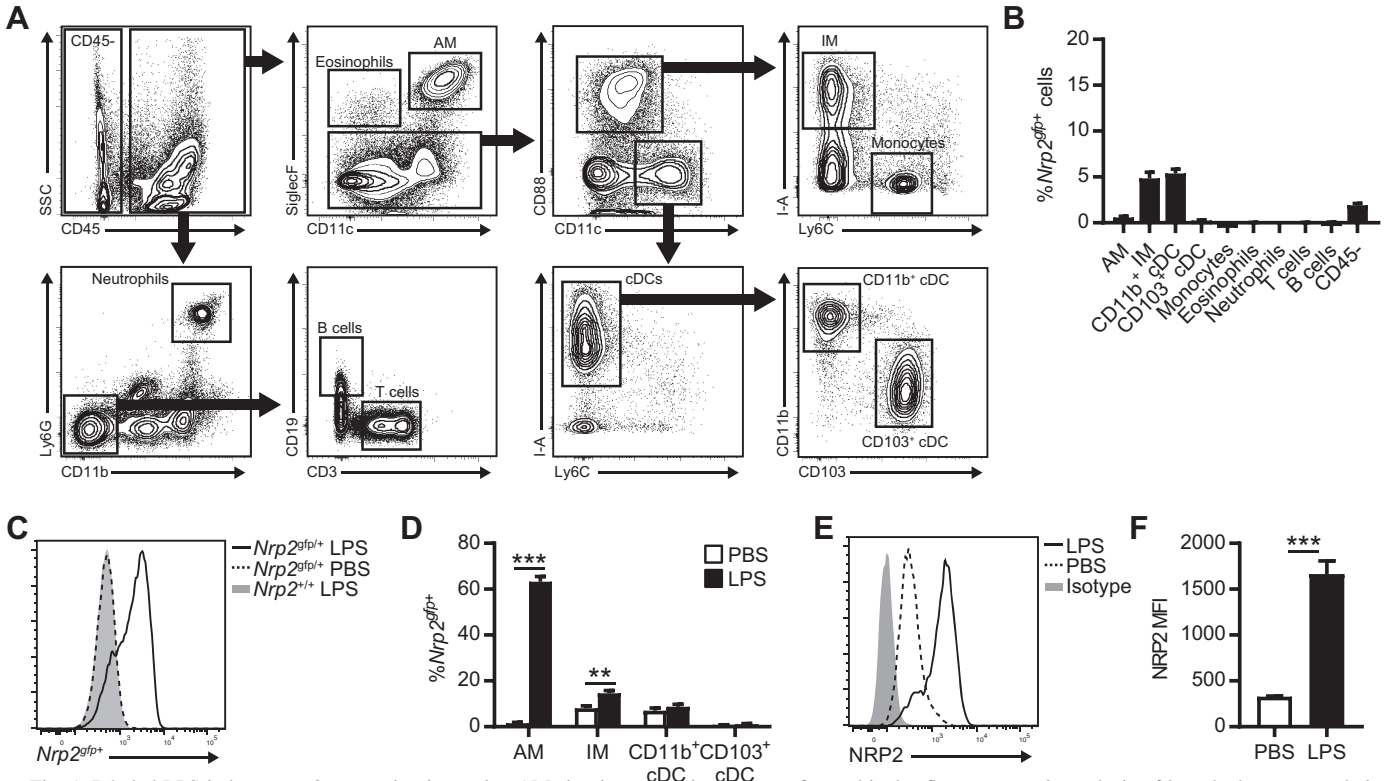

Fig. 1. Inhaled LPS induces *Nrp2* expression in murine AMs in vivo. *A*: gating strategy for multicolor flow cytometric analysis of lung leukocyte populations. *B*: quantitation of $Nrp2^{gfp}$ expression by lung cells from untreated $Nrp2^{gfp/+}$ reporter mice. Bars represent means ± SE (n ± 6 mice/group). *C* and *D*: flow cytometric analysis of $Nrp2^{gfp}$ expression by AMs from $Nrp2^{gfp/+}$ mice at 16 h after airway instillation of LPS or PBS. *C*: representative histograms showing $Nrp2^{gfp}$ expression by AMs from $Nrp2^{gfp/+}$ mice treated with LPS (solid line) or PBS (dashed line). AMs from LPS-treated $Nrp2^{+/+}$ were included as a negative control for $Nrp2^{gfp}$ fluorescence (gray histogram). *D*: quantitation of $Nrp2^{gfp}$ expression by lung macrophages and DCs at 16 h after airway instillation of LPS or PBS. Bars represent means ± SE (n ± 5–6 mice/group). *E* and *F*: low cytometric analysis of NRP2 surface protein expression by AMs from C57BL/6 mice at 16 h after airway instillation of LPS or PBS. *E*: representative histograms of NRP2 surface protein expression by AM from mice treated with LPS (solid line) or PBS (dashed line). Cells stained with goat IgG served as the isotype control (gray histogram). *F*: median fluorescent intensity (MFI) of NRP2 staining of AMs from PBS- or LPS-treated. Bars represent means NRP2 MFI ± SE (n ± 4 mice/group). $^{**}P$ ± 0.01, $^{***}P$ ± 0.001, Student's *t*-test. AMs, alveolar macrophages; NRP2, neuropilin-2; DC, dendritic cell; IM, interstitial macrophage.

able in the cytoplasm and plasma membrane of AMs at 24-h post-LPS treatment (Fig. 2*A*). To quantify NRP2 protein expression by human AMs more accurately, we analyzed NRP2 cell surface display by flow cytometry. The mean fluorescence intensity for NRP2 antibody staining was significantly increased in LPS-treated human AMs compared with untreated cells, indicating increased amounts of cell surface protein (Fig. 2, *B* and *C*). Finally, we analyzed *NRP2* mRNA expression in LPS-treated human AMs by quantitative PCR analysis at 6-h post-LPS treatment. *NRP2* mRNA expression was ~1.5-fold higher in LPS-treated AMs than in PBS-treated AM (Fig. 2*D*). Thus, ex vivo stimulation of human AMs with LPS induces NRP2 protein and mRNA expression.

Nrp2 induction by LPS is dependent on MyD88 and NF-κB signaling pathways. Activation of TLR4 by LPS initiates signaling pathways downstream of either MyD88 or TIR-domain-containing adapter-inducing interferon-β adapter proteins, resulting in nuclear translocation of transcription factors and gene transcription (1). We therefore investigated whether *Nrp2* gene expression by LPS-stimulated AMs was dependent on MyD88 and/or TIR-domain-containing adapter-inducing interferon-β signaling pathways. AMs were harvested from wild-type (C57BL/6), *Myd88*$^{-/-}$, or *Trif*$^{-/-}$ mice and stimulated with LPS. LPS-induced *Nrp2* expression was completely abrogated in *Myd88*$^{-/-}$ AMs (Fig. 3*A*), indicating that MyD88-dependent signaling is essential for *Nrp2* gene transcription following TLR4 activation. By contrast, AMs from *Trif*$^{-/-}$ mice upregulated *Nrp2* following LPS stimulation, albeit at a reduced level compared with wild-type AMs (Fig. 3*A*). Therefore, *Nrp2* gene expression following LPS stimulation is primarily mediated by the MyD88-dependent signaling pathway.

Recruitment of MyD88 to the TLR complex initiates downstream signaling pathways that results in activation of transcription factors including NF-κB (1). Nuclear translocation of NF-κB leads to transcription of several genes involved with immune regulation, but whether *Nrp2* expression is NF-κB-dependent is unknown. To address this, we evaluated *Nrp2* mRNA in AMs stimulated with LPS in the presence of the selective NF-κB inhibitor, PDTC. PDTC treatment of AMs completely abolished LPS-induced *Nrp2* expression (Fig. 3*B*). As expected, PDTC treatment also prevented induction of the NF-κB-dependent gene *Il6* (Fig. 3*B*). However, PDTC treatment did not affect expression of the constitutively expressed gene *Ppih* (Fig. 3*B*), indicating that PDTC did not globally inhibit gene transcription in AMs. To verify that LPS-induced *Nrp2* expression was dependent on NF-kB, we also analyzed *Nrp2* gene expression in AMs treated with the IKK inhibitor BMS-345541. Consistent with our findings in PDTC-treated AMs, treatment of AMs with BMS-345541 also suppressed *Nrp2* gene expression following LPS stimulation (Fig. 3*C*). Taken together, these data show that LPS-induced *Nrp2* expression in AMs is dependent on MyD88 and NF-κB signaling pathways.

LPS inhalation triggers release of sNRP2 into the airways. NRP2 exists in both transmembrane and soluble forms (40). sNRP2 can be produced either by alternative mRNA splicing or by ectodomain shedding of the transmembrane protein (40, 47). sNRP2 has been detected in serum (14) and synovial fluid (13), but whether it is also present in the respiratory tract is unknown. Using immunoblot analysis, we investigated whether sNRP2 was present in murine BAL fluid following airway instillation of PBS or LPS. Immunoblot analysis for NRP2 in BAL fluid from PBS- and LPS-treated mice revealed a soluble isoform of ~110 kDa. sNRP2 was barely detectable in BAL fluid from PBS-treated mice (Fig. 4*A*), indicating that sNRP2 was present at low levels in murine airways under steady-state conditions. By contrast, sNRP2 was readily detected in BAL fluid from LPS-treated mice (Fig. 4*A*). Quantification of sNRP2 protein by densitometry showed that sNRP2 levels in BAL fluid were significantly increased following LPS inhalation (Fig. 4*B*). Thus, LPS inhalation induces expression of both transmembrane and soluble forms of NRP2 in the airways.

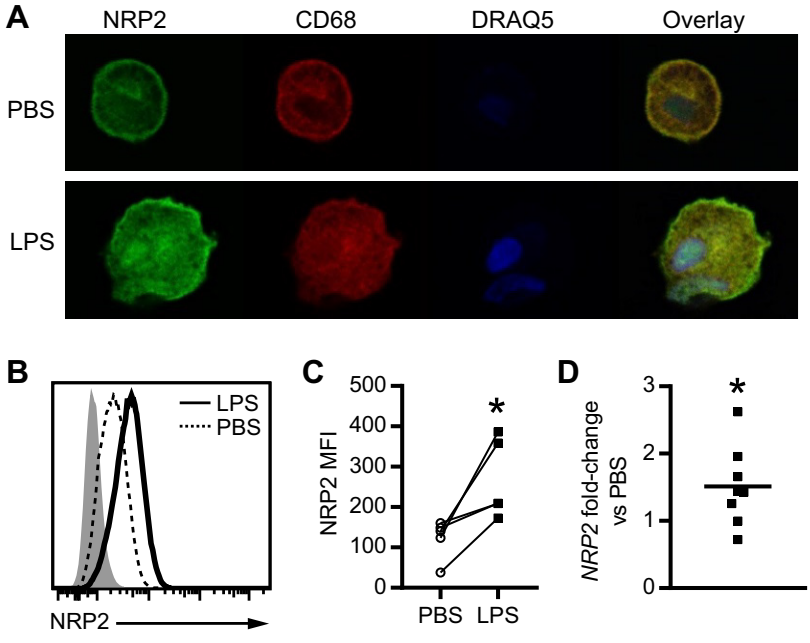

Fig. 2. NRP2 is upregulated by human AMs following ex vivo LPS stimulation. Human AMs from healthy volunteers were treated with LPS (100 ng/ml) or PBS for 24 (*A–C*) or 6 (*D*) h. Immunofluorescence confocal microscopic images show PBS- or LPS-treated human AMs stained with NRP2 antibody (green), CD68 antibody (red), or the nuclear stain DRAQ5 (blue) (*A*). Images are representative of data obtained from AM from 3 separate volunteers. Representative histograms depicting NRP2 cell surface display on human AMs treated with LPS (solid line) or PBS (dashed line) for 24 h (*B*). AMs stained with goat IgG served as the isotype control (gray histogram). MFI of NRP2 antibody staining of human AMs ($n = 5$ volunteers) treated with PBS or LPS (*C*). *$P < 0.05$, paired *t*-test. Quantitative PCR analysis of *Nrp2* mRNA expression by human AMs stimulated with LPS for 6 h (*D*). Bar represents means ($n = 8$ volunteers) of the fold-change relative to AMs treated with PBS. *$P < 0.05$, Student's *t*-test (compared with media-treated AMs). AMs, alveolar macrophages; MFI, mean fluorescent intensity; NRP2, neuropilin-2.

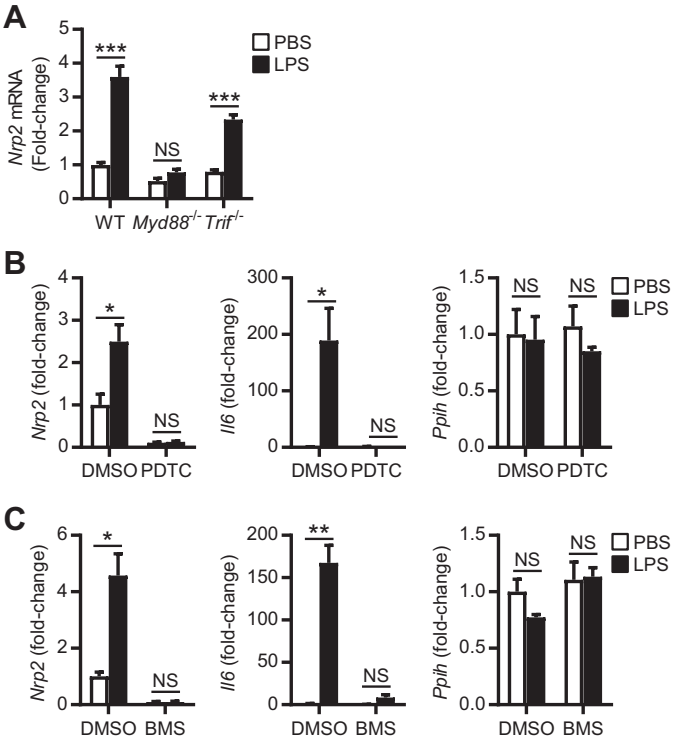

Fig. 3. LPS-induced *Nrp2* expression by AMs is dependent upon MyD88 and NF-κB. AMs from C57BL/6 wild-type (WT), *Myd88*$^{-/-}$, or *Trif*$^{-/-}$ mice were treated with LPS or PBS (*A*). Six hours later, the fold-change of *Nrp2* mRNA expression (relative to PBS-treated WT AMs) was determined by qPCR. Bars represent mean ± SE (n = 4 mice/group). Representative data from 1 of 2 independent experiments are shown. AMs from C57BL/6 mice were pretreated with DMSO, the NF-κB inhibitor PDTC (*B*), or the IKK inhibitor BMS-345541 (BMS) (*C*) for 1 h and then treated with PBS or LPS. Six hours later, the fold-change of *Nrp2*, *Il6*, *and Ppih* mRNA expression (relative to PBS/DMSO-treated AMs) was determined by qPCR. Bars represent means ± SE (n = 3–4 mice/group). Representative data from 1 of 2 independent experiments are shown. $^{*}P < 0.05$, $^{**}P < 0.01$, $^{***}P < 0.001$, Student's t-test. AMs, alveolar macrophages; DMSO, dimethyl sulfoxide; MyD88, myeloid differentiation primary response 88; NRP2, neuropilin-2; NS, not significant; PDTC, pyrrolidinedithiocarbamate; qPCR, quantitative PCR.

AMs are the primary source of sNRP2 in the airways. LPS has been reported to trigger shedding of sNRP2 by murine microglia (47), but whether AMs also release sNRP2 is unknown. To investigate this, we first analyzed supernatants from ex vivo cultured murine AMs for the presence of sNRP2. Similar to BAL fluid, culture supernatants from LPS-treated AMs contained a ~110-kDa soluble isoform of NRP2 (Fig. 5*A*). A weaker band was also present in PBS-treated AMs, which was likely due to spontaneous activation of AMs during ex vivo culture. In comparison, cell lysates from PBS- or LPS-treated AMs contained the full-length ~140-kDa isoform of murine NRP2 (Fig. 5*A*). Thus, AMs are capable of producing sNRP2 after ex vivo stimulation.

We next investigated whether AMs are the source of sNRP2 in the respiratory tract in vivo. For this, we crossed conditionally mutant *Nrp2*-floxed (*Nrp2*$^{fl/fl}$) mice with transgenic mice expressing Cre recombinase under control of the *Lyz2* gene promoter (LysMcre) to generate myeloid-specific *Nrp2* knockout mice (LysMcre/*Nrp2*$^{fl/fl}$). As expected, *Nrp2* mRNA and protein expression were absent in AMs from LysMcre/*Nrp2*$^{fl/fl}$ (Fig. 5*B*), confirming efficient Cre-mediated recombination at the *Nrp2* locus in AMs. We then challenged LysMcre/*Nrp2*$^{fl/fl}$ and control *Nrp2*$^{fl/fl}$ mice with inhaled LPS and analyzed BAL fluid for sNRP2 by immunoblot. As expected, inhaled LPS resulted in increased sNRP2 protein levels in BAL fluid from *Nrp2*$^{fl/fl}$ mice (Fig. 5*C*). By contrast, sNRP2 was not detected in BAL fluid from either PBS- or LPS-treated LysMcre/*Nrp2*$^{fl/fl}$ mice (Fig. 5*C*). Because *Nrp2* is not significantly expressed by other myeloid cells in the lungs (Fig. 1, *B* and *C*), our findings suggest that AMs are primarily responsible for the production of sNRP2 in the respiratory tract.

Myeloid-specific ablation of NRP2 results in prolonged LPS-induced airway inflammation. The observed induction of transmembrane and soluble NRP2 expression by AMs following LPS treatment suggested that NRP2 may be important in regulating airway inflammatory responses. To investigate this possibility, we compared LPS-induced airway inflammation in *Nrp2*$^{fl/fl}$ and LysMcre/*Nrp2*$^{fl/fl}$ mice. At *day 1* post-LPS treatment, BAL leukocytes were similarly increased in both *Nrp2*$^{fl/fl}$ and LysMcre/*Nrp2*$^{fl/fl}$ mice compared with PBS-treated mice (Fig. 6, *A* and *C*). However, LysMcre/*Nrp2*$^{fl/fl}$ mice demonstrated a persistent increase in total BAL leukocytes when compared with *Nrp2*$^{fl/fl}$ mice at *day 4* post-LPS treatment (Fig. 6*A*). Histological analysis of lungs at *day 4* post-LPS treatment also demonstrated persistent leukocyte infiltrates in LysMcre/*Nrp2*$^{fl/fl}$ mice (Fig. 6*B*). The increase in total airway leukocytes at *day 4* post-LPS was due to elevated numbers of monocyte/macrophages and neutrophils in the BAL (Fig. 6*C*). Total BAL protein levels also remained elevated in LysMcre/*Nrp2*$^{fl/fl}$ mice on *day 4* post-LPS (Fig. 6*D*), suggesting increased vascular permeability following LPS exposure. Both *Nrp2*$^{fl/fl}$ and LysMcre/*Nrp2*$^{fl/fl}$ mice had similar numbers of BAL cells by 7 days post-LPS treatment (Fig. 6, *A* and *C*), suggesting that the regulatory activity of NRP2 was most important during the early stages of the airway inflammatory response. To investigate the mechanism responsible for the increased number of airway inflammatory cells in LysMcre/*Nrp2*$^{fl/fl}$ mice following

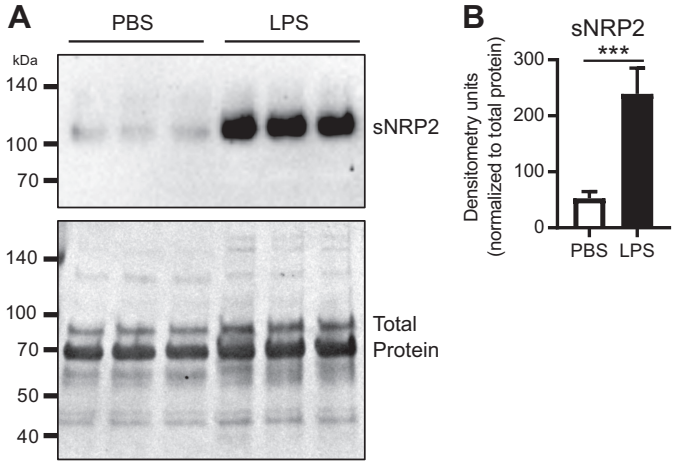

Fig. 4. Inhaled LPS triggers release of soluble NRP2 (sNRP2) into the airways. *A*: bronchoalveolar lavage fluid (BALF) from C57BL/6 mice was collected 24 h after airway administration of PBS or LPS and analyzed by immunoblotting for NRP2 (*top*). Representative data from 3 mice/treatment group are presented. Coomassie staining of the membrane was performed as a control for gel loading and protein transfer (*bottom*). *B*: quantitation of sNRP2 in BALF by immunoblot densitometry. Bars represent means ± SE (n = 8–10 mice/group). $^{***}P < 0.001$, Mann-Whitney test. NRP2, neuropilin-2.

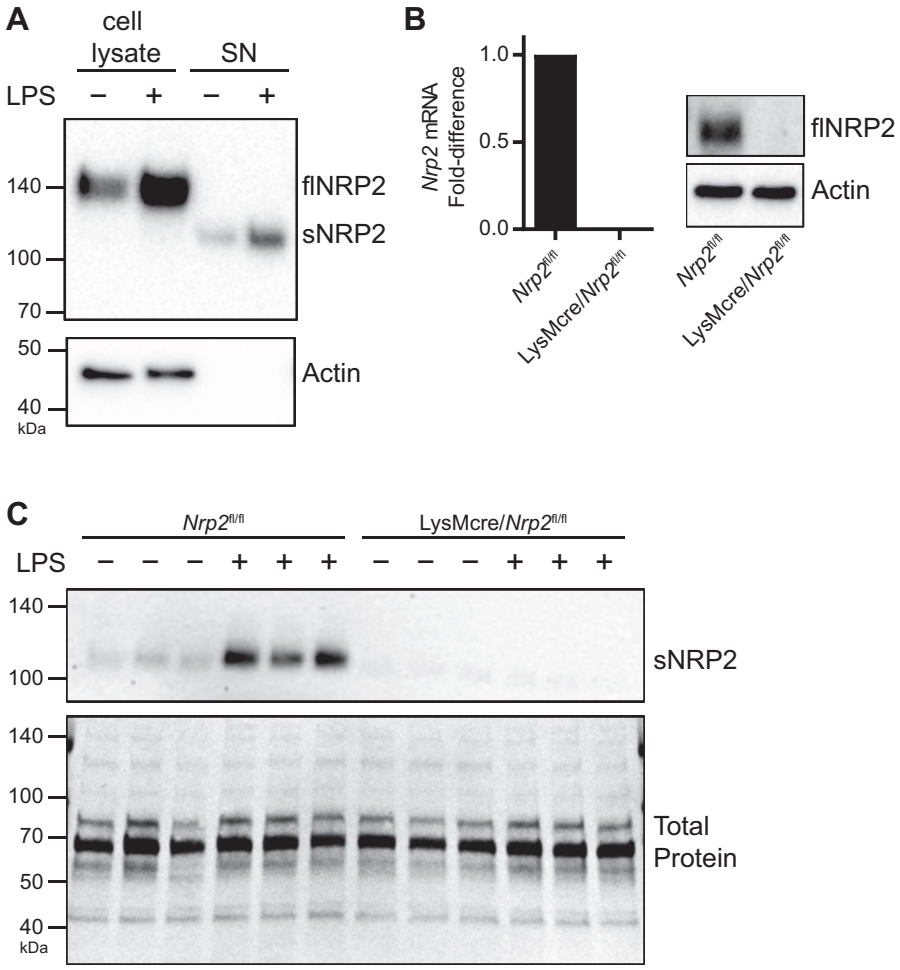

Fig. 5. AMs are the source of sNRP2 in the airways. *A*: AM from C57BL/6 were treated ex vivo with LPS or PBS. After 24 h, cell lysates and culture supernatants (SN) were collected and analyzed by immunoblot for full-length (flNRP2) and sNRP2. Immunoblot for actin was performed as a control for protein loading of cell lysates and as a marker of cell death in SN. Data are from 1 experiment, representative of 3. *B*: AMs from *Nrp2*$^{fl/fl}$ and LysMcre/*Nrp2*$^{fl/fl}$ mice were treated ex vivo with LPS. After 24 h, AMs were analyzed by qPCR for *Nrp2* mRNA expression (*left*) or immunoblot for flNRP2 protein (*right*). *C*: BALF from *Nrp2*$^{fl/fl}$ and LysMcre/*Nrp2*$^{fl/fl}$ mice (n = 3 mice/group) was collected 24 h after airway administration of PBS or LPS and analyzed for the presence of sNRP2 by immunoblotting. Coomassie staining of the membrane was performed as a control for gel loading and protein transfer (*bottom*). Representative data from 1 of 2 experiments are shown. AMs, alveolar macrophages; BALF, bronchoalveolar lavage fluid; NRP2, neuropilin-2; sNRP2, soluble NRP2; qPCR, quantitative PCR.

LPS treatment, we analyzed inflammatory chemokine expression in the lungs at *days 1* and *4* post-LPS treatment (Fig. 6*E*). On *days 1* and *4* post-LPS treatment, the neutrophil chemokines *Cxcl1* and *Cxcl2* were expressed at similar levels, whereas there was a trend toward increased *Cxcl5* expression in the lungs of LysMcre/*Nrp2*$^{fl/fl}$ mice on *day 4* post-LPS treatment (Fig. 6*E*). By contrast, LysMcre/*Nrp2*$^{fl/fl}$ mice had significantly higher lung *Ccl2* expression compared with *Nrp2*$^{fl/fl}$ mice on *day 4* post-LPS treatment (Fig. 6*E*), which coincided with increased numbers of BAL leukocytes (Fig. 6, *A* and *C*). *Nrp2*$^{fl/fl}$ and LysMcre/*Nrp2*$^{fl/fl}$ mice had similar lung *Ccl2* expression on *day 1* post-LPS treatment, indicating that NRP2 did not regulate early induction of *Ccl2* by LPS but may be involved with downregulation of *Ccl2* expression during resolution of lung inflammation. In summary, conditional ablation of NRP2 in myeloid cells results in prolonged leukocyte accumulation in the lungs following LPS inhalation, which was associated with increased *Ccl2* mRNA expression in lung tissue.

DISCUSSION

Recognition of PAMPs by the innate immune system is essential for the rapid identification and elimination of inhaled pathogens (50). However, innate immune responses to inhaled PAMPs can also lead to immune-mediated lung injury and impairment (24). Moreover, activation of TLR by inhaled PAMPs can exacerbate underlying inflammatory lung diseases such as asthma and chronic obstructive pulmonary disease (11, 52). Therefore, innate immune responses in the airways must be tightly regulated to prevent deleterious inflammation. Here, we provide evidence that NRP2 expression by AMs is important for regulating inflammatory responses to inhaled LPS at levels similar to what might be encountered in high-endotoxin work environments (12). We found that LPS induces NRP2 expression in murine and human AMs, and that this induction is dependent upon the MyD88-NF-κB signaling pathway. We also discovered that LPS inhalation triggers AMs to release a soluble form of NRP2 into the airways. Finally, we found that myeloid-specific ablation of NRP2 results in prolonged LPS-induced airway inflammation. Overall, these findings support an inhibitory role for NRP2 in LPS-induced airway inflammation.

Although originally described for its role in axonal guidance, there is growing evidence that NRP2 may be important in regulating innate immune responses (41, 42). For example, NRP2 deficiency results in exaggerated cutaneous inflammation in a delayed-type hypersensitivity mouse model (34). Furthermore, NRP2-deficient mice have enhanced LPS-induced inflammation of the cornea (46). Recently, immunohistochemistry analysis of human lung tissue revealed NRP2 expression in AMs and bronchial macrophages (2), suggesting that NRP2 may play a role in lung innate immunity. Using

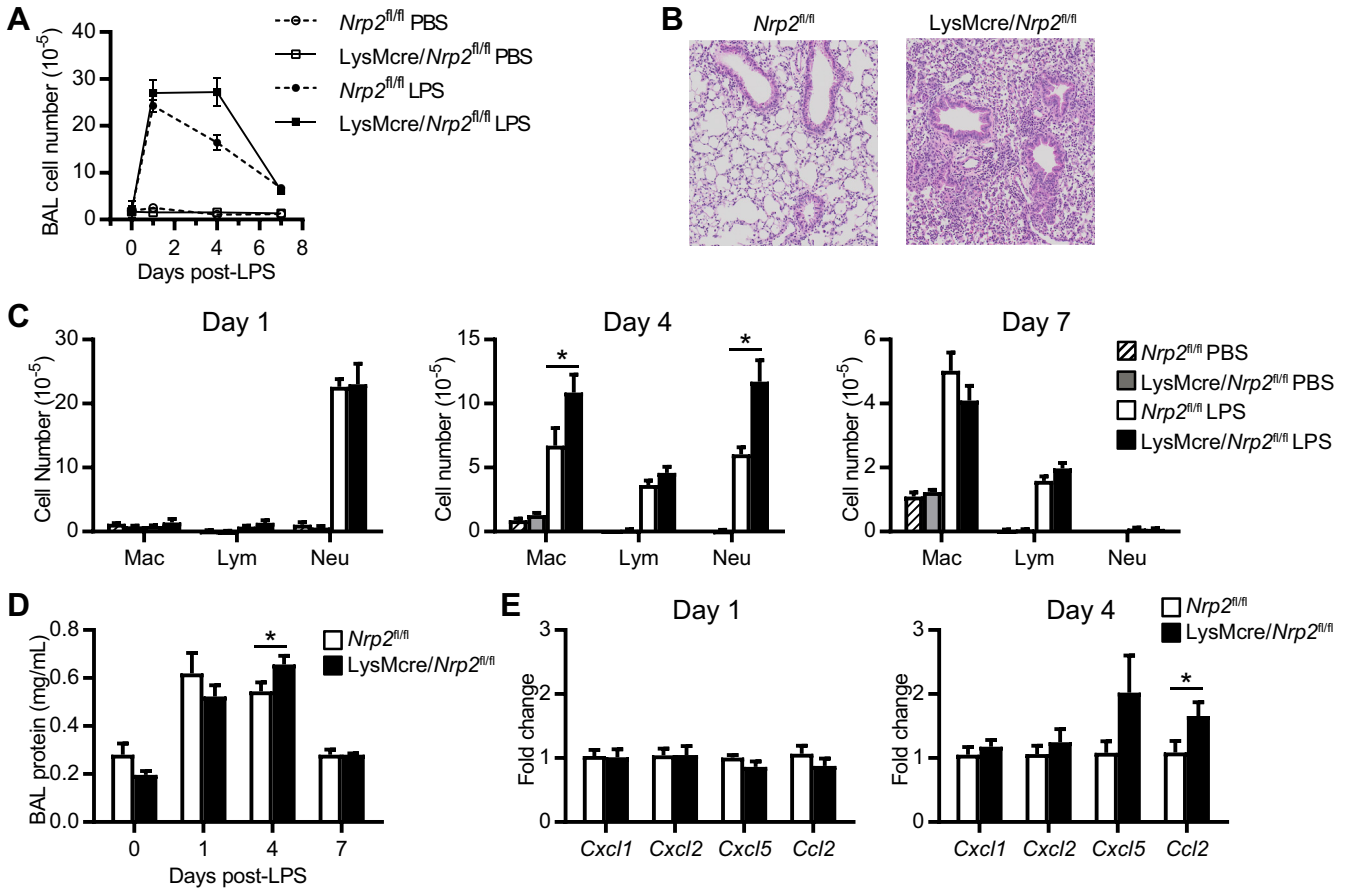

Fig. 6. Myeloid-specific ablation of NRP2 results in prolonged LPS-induced airway inflammation. *A*: LPS or PBS was administered to the airways of *Nrp2*$^{fl/fl}$ or LysMcre/*Nrp2*$^{fl/fl}$ mice. BALF and lung tissue were collected at 1, 4, and 7 days posttreatment, and cell counts and differentials were determined. Symbols represent means ± SE (n = 8–9 mice/time point for LPS-treated mice; n = 3–4 mice/time point for PBS-treated mice). *B*: representative hematoxylin and eosin staining of lungs from *Nrp2*$^{fl/fl}$ and LysMcre/*Nrp2*$^{fl/fl}$ mice at *day 4* post-LPS treatment. *C*: number of macrophages (Mac), lymphocytes (Lym), and neutrophils (Neu) in BALF on *days 1*, *4*, and *7* posttreatment with either PBS or LPS. Bars represent the mean ± SE (n = 8–9 mice/time point for LPS-treated mice; n = 3–4 mice/time point for PBS-treated mice). *D*: total BALF protein at *day 4* post-LPS treatment. Bars represent means ± SE (n = 8–9 mice/group). *E*: chemokine mRNA expression in lung homogenates at *days 1* and *4* post-LPS treatment. Results for each chemokine are presented as fold-change relative to expression in *Nrp2*$^{fl/fl}$ mice. Bars represent means ± SE (n = 8–9 mice/group). *$P < 0.05$, Mann-Whitney test. BALF, bronchoalveolar lavage fluid; NRP2, neuropilin-2.

freshly isolated BAL cells from normal donors, we confirmed NRP2 expression in human AMs at both the protein and transcriptional levels. Similarly, we observed detectable but low-level expression of *Nrp2* in murine AMs under steady-state conditions. By contrast, LPS-mediated activation of both human and murine AMs significantly upregulated NRP2 mRNA and cell-surface protein expression. In addition, LPS triggered the release of soluble NRP2 by murine AMs both ex vivo and in vivo. Given the importance of AMs in maintaining immune homeostasis (21), it is possible that induction of *NRP2* expression by LPS may serve as a negative regulator of airway inflammation. Consistent with this notion, myeloid-specific ablation of NRP2 resulted in prolonged accumulation of airway leukocytes following acute LPS exposure. The accumulation of airway leukocytes was associated with significantly increased *Ccl2* mRNA expression in the lungs of LysMcre/*Nrp2*$^{fl/fl}$ mice at *day 4* post-LPS treatment. Although we did not detect increased CCL2 protein in BAL fluid from LysMcre/*Nrp2*$^{fl/fl}$ mice (data not shown), it is likely that increased *Ccl2* mRNA expression leads to elevated levels of CCL2 in the lung interstitium, thereby contributing to recruitment of CCR2^{+} monocytes and macrophages to the airways during inflammation (28). Furthermore, CCL2-mediated monocyte accumulation has been reported to promote neutrophil migration to the alveolar space (28, 29), which may explain the persistence of neutrophils in the airways of LysMcre/*Nrp2*$^{fl/fl}$ mice at *day 4* post-LPS treatment. It is possible that NRP2 may directly regulate LPS-induced *Ccl2* expression by lung macrophages. In support of this, the related molecule NRP1 has been shown to inhibit TLR signaling in macrophages (10) and DCs (37). However, we did not observe increased *Ccl2* expression in NRP2-deficient AMs stimulated ex vivo with LPS (data not shown), suggesting that unlike NRP1, NRP2 does not regulate TLR signaling in myeloid cells. Alternatively, sNRP2 produced by AMs may inhibit *Ccl2* expression by other cell types, such as airway epithelial cells (3). Further studies are needed to determine how CCL2 contributes to the prolonged airway inflammatory response observed in LysMcre/*Nrp2*$^{fl/fl}$ mice.

In addition to enhanced leukocyte accumulation in the airways, myeloid-specific ablation of NRP2 also resulted in a persistent increase in total protein levels in BAL fluid following LPS inhalation, suggesting that NRP2 may regulate pulmonary vascular permeability. NRP2-deficient mice have previously been reported to have increased vascular permeability

during inflammation (34), but how myeloid-specific production of NRP2 regulates vascular integrity is unclear. As has been described for soluble NRP1 (15), it is possible that release of sNRP2 by AMs may bind to and inhibit VEGF-A, which is an important mediator of vascular permeability in the lung (30). Alternatively, loss of NRP2 signaling in AMs may disrupt AM-epithelial cell interactions, which is critical for regulating inflammatory responses to inhaled microbial products (5). Indeed, NRP2 has been reported to interact with integrins and facilitate formation of focal cell adhesions (17). Moreover, NRP2 signaling regulates F-actin reorganization in immune cells (9), which could also impact cell adhesion. Further studies are needed to delineate the role of myeloid-derived NRP2 in regulating vascular permeability in the lungs.

The transcriptional regulation of *Nrp2* in macrophages has not been previously characterized. Our observation that TLR activation induced *Nrp2* expression in AMs suggested a potential role of NF-κB in positively regulating *Nrp2* transcription. Indeed, we found that inhibition of NF-κB completely abolished LPS-induced *Nrp2* expression in murine AMs. Interestingly, NF-κB has been shown to repress expression of *Nrp1* in macrophages (10), indicating that neuropilin family members are differentially regulated by NF-κB. The biological significance of this is unclear but suggests that NRP1 and NRP2 have distinct roles in regulating macrophage function. Although LPS-induced *Nrp2* expression is dependent on NF-κB, it is likely that other transcription factors are involved with regulating baseline expression of *Nrp2* in AMs. Possible candidates include GATA-binding protein 2 and LIM domain only 2, which have been reported to regulate *NRP2* expression in endothelial cells (7). Whether these transcription factors also regulate *NRP2* expression in macrophages requires additional study.

NRP1 and NRP2 are reported to have both transmembrane and soluble forms (40). A soluble isoform of sNRP2 can be generated by ectodomain shedding of transmembrane NRP2 on human and mouse myeloid cells (47). Additionally, a soluble splice form of human NRP2 has been identified at the transcript level in humans (40) but not in mice. sNRP2 has been detected in synovial fluid and serum (13, 14), but whether it is expressed in the respiratory tract has not been previously addressed. Here, we report for the first time that sNRP2 is present in the murine airway. Airway levels of sNRP2 were low under steady-state conditions but significantly increased after LPS inhalation. Using conditional knockout mice and ex vivo AM cultures, we provide strong evidence that AMs are the primary source of sNRP2 in the respiratory tract. The molecular mass of sNRP2 in BAL fluid and AM cell culture supernatants was ~110 kDa, suggesting that it was the product of ectodomain shedding. It was recently reported that shedding of sNRP2 from microglia was dependent upon LPS-induced metalloproteinase activity (47). Because LPS inhalation can increase metalloproteinases in BAL fluid (16), it is possible that release of sNRP2 into the airways following LPS challenge is also metalloproteinase-dependent. Alternatively, murine AMs could produce a novel soluble NRP2 isoform by alternative splicing of the *Nrp2* gene. The mechanism by which murine AMs produce sNRP2 requires further study.

The functional importance of sNRP2 is in the airway is unknown. As mentioned previously, soluble NRP1 is an endogenous inhibitor of VEGF-A (15), suggesting that sNRP2 may also antagonize VEGF signaling. Indeed, a recombinant sNRP2 construct (containing only the ligand-binding coagulation factor domains) was recently shown to be a potent inhibitor of VEGF-C in vitro (38), but whether naturally occurring sNRP2 inhibits VEGF signaling in vivo is unknown. Given the role of VEGF in airway inflammation and remodeling (32), it is conceivable that sNRP2 is an important regulator of VEGF activity in the lungs. Alternatively, polysialylated sNRP2 may act as an anti-inflammatory mediator in the airways. By binding to sialic acid-binding immunoglobulin-like lectin 11 receptor on human myeloid cells, polysialic acid can inhibit LPS-induced inflammatory responses (43). Furthermore, nanoparticles coated with polysialic acid residues were shown to attenuate pulmonary inflammation in an LPS-mediated lung injury model (44). Thus, it will be important to determine if sNRP2 in the airways is polysialylated and if this posttranslational modification is necessary for the immunomodulatory properties of NRP2.

In summary, we have shown that LPS induces NRP2 expression in both human and murine AMs. NRP2 induction is dependent upon the MyD88-NF-κB signaling pathway. In addition, we have described for the first time the presence of sNRP2 in the respiratory tract, and that AMs are the primary source for sNRP2 in the airways. Importantly, myeloid-specific ablation of NRP2 results in prolonged LPS-induced airway inflammation. Overall, our findings indicate that NRP2 is an important regulator of immune responses to inhaled microbial products and provide the rationale for future studies investigating the role of NRP2 in inflammatory lung diseases.

ACKNOWLEDGMENTS

We thank Tongde Wu, Michael Chua, and Rob Tarran for assistance with confocal microscopy and immunoblot analysis; Joleen Soukup for preparation of human alveolar macrophages; and Kim Burns in the Marsico Lung Institute Histology Core for preparation of lung histology sections.

GRANTS

This work was supported by the Intramural Research Program of the National Institutes of Health, the National Institute of Environmental Health Sciences (ZIA ES-102025-09); the North Carolina Children's Promise Grant; the American Academy of Allergy, Asthma and Immunology Foundation Inc.; and the National Center for Advancing Translational Sciences, National Institutes of Health (1KL2TR001109).

DISCLOSURES

No conflicts of interest, financial or otherwise, are declared by the authors.

AUTHOR CONTRIBUTIONS

D.N.C. and T.P.M. conceived and designed research; R.M.I., D.C.L., and T.P.M. performed experiments; D.N.C. and T.P.M. analyzed data; H.N., M.L.H., N.E.A., A.J.G., S.L.T., C.M.D., D.B.P., D.N.C., and T.P.M. interpreted results of experiments; T.P.M. prepared figures; T.P.M. drafted manuscript; R.M.I., H.N., N.E.A., A.J.G., D.N.C., and T.P.M. edited and revised manuscript; R.M.I., D.C.L., H.N., M.L.H., N.E.A., A.J.G., S.L.T., C.M.D., D.B.P., D.N.C., and T.P.M. approved final version of manuscript.

REFERENCES

1. **Akira S, Takeda K.** Toll-like receptor signalling. *Nat Rev Immunol* 4: 499–511, 2004. doi:10.1038/nri1391.
2. **Aung NY, Ohe R, Meng H, Kabasawa T, Yang S, Kato T, Yamakawa M.** Specific neuropilins expression in alveolar macrophages among tissue-specific macrophages. *PLoS One* 11: e0147358, 2016. doi:10.1371/journal.pone.0147358.
3. **Becker S, Quay J, Koren HS, Haskill JS.** Constitutive and stimulated MCP-1, GRO alpha, beta, and gamma expression in human airway

epithelium and bronchoalveolar macrophages. *Am J Physiol* 266: L278–L286, 1994. doi:10.1152/ajplung.1994.266.3.L278.
4. **Bhat TA, Panzica L, Kalathil SG, Thanavala Y.** Immune dysfunction in patients with chronic obstructive pulmonary disease. *Ann Am Thorac Soc* 12, *Suppl* 2: S169–S175, 2015. doi:10.1513/AnnalsATS.201503-126AW.
5. **Bhattacharya J, Westphalen K.** Macrophage-epithelial interactions in pulmonary alveoli. *Semin Immunopathol* 38: 461–469, 2016. doi:10.1007/s00281-016-0569-x.
6. **Chen H, Chédotal A, He Z, Goodman CS, Tessier-Lavigne M.** Neuropilin-2, a novel member of the neuropilin family, is a high affinity receptor for the semaphorins Sema E and Sema IV but not Sema III. *Neuron* 19: 547–559, 1997. doi:10.1016/S0896-6273(00)80371-2.
7. **Coma S, Allard-Ratick M, Akino T, van Meeteren LA, Mammoto A, Klagsbrun M.** GATA2 and Lmo2 control angiogenesis and lymphangiogenesis via direct transcriptional regulation of neuropilin-2. *Angiogenesis* 16: 939–952, 2013. doi:10.1007/s10456-013-9370-9.
8. **Curreli S, Arany Z, Gerardy-Schahn R, Mann D, Stamatos NM.** Polysialylated neuropilin-2 is expressed on the surface of human dendritic cells and modulates dendritic cell-T lymphocyte interactions. *J Biol Chem* 282: 30346–30356, 2007. doi:10.1074/jbc.M702965200.
9. **Curreli S, Wong BS, Latinovic O, Konstantopoulos K, Stamatos NM.** Class 3 semaphorins induce F-actin reorganization in human dendritic cells: Role in cell migration. *J Leukoc Biol* 100: 1323–1334, 2016. doi:10.1189/jlb.2A1114-534R.
10. **Dai X, Okon I, Liu Z, Wu Y, Zhu H, Song P, Zou MH.** A novel role for myeloid cell-specific neuropilin 1 in mitigating sepsis. *FASEB J* 31: 2881–2892, 2017. doi:10.1096/fj.201601238R.
11. **Doreswamy V, Peden DB.** Modulation of asthma by endotoxin. *Clin Exp Allergy* 41: 9–19, 2011. doi:10.1111/j.1365-2222.2010.03628.x.
12. **Duquenne P, Marchand G, Duchaine C.** Measurement of endotoxins in bioaerosols at workplace: a critical review of literature and a standardization issue. *Ann Occup Hyg* 57: 137–172, 2013. doi:10.1093/annhyg/mes051.
13. **Fassold A, Falk W, Anders S, Hirsch T, Mirsky VM, Straub RH.** Soluble neuropilin-2, a nerve repellent receptor, is increased in rheumatoid arthritis synovium and aggravates sympathetic fiber repulsion and arthritis. *Arthritis Rheum* 60: 2892–2901, 2009. doi:10.1002/art.24860.
14. **Fung TM, Ng KY, Tong M, Chen JN, Chai S, Chan KT, Law S, Lee NP, Choi MY, Li B, Cheung AL, Tsao SW, Qin YR, Guan XY, Chan KW, Ma S.** Neuropilin-2 promotes tumourigenicity and metastasis in oesophageal squamous cell carcinoma through ERK-MAPK-ETV4-MMP-E-cadherin deregulation. *J Pathol* 239: 309–319, 2016. doi:10.1002/path.4728.
15. **Gagnon ML, Bielenberg DR, Gechtman Z, Miao HQ, Takashima S, Soker S, Klagsbrun M.** Identification of a natural soluble neuropilin-1 that binds vascular endothelial growth factor: In vivo expression and antitumor activity. *Proc Natl Acad Sci USA* 97: 2573–2578, 2000. doi:10.1073/pnas.040337597.
16. **Gibbs DF, Shanley TP, Warner RL, Murphy HS, Varani J, Johnson KJ.** Role of matrix metalloproteinases in models of macrophage-dependent acute lung injury. Evidence for alveolar macrophage as source of proteinases. *Am J Respir Cell Mol Biol* 20: 1145–1154, 1999. doi:10.1165/ajrcmb.20.6.3482.
17. **Goel HL, Pursell B, Standley C, Fogarty K, Mercurio AM.** Neuropilin-2 regulates α6β1 integrin in the formation of focal adhesions and signaling. *J Cell Sci* 125: 497–506, 2012. doi:10.1242/jcs.094433.
18. **Guo HF, Vander Kooi CW.** Neuropilin functions as an essential cell surface receptor. *J Biol Chem* 290: 29120–29126, 2015. doi:10.1074/jbc.R115.687327.
19. **Han S, Mallampalli RK.** The acute respiratory distress syndrome: from mechanism to translation. *J Immunol* 194: 855–860, 2015. doi:10.4049/jimmunol.1402513.
20. **Holgate ST.** Innate and adaptive immune responses in asthma. *Nat Med* 18: 673–683, 2012. doi:10.1038/nm.2731.
21. **Hussell T, Bell TJ.** Alveolar macrophages: plasticity in a tissue-specific context. *Nat Rev Immunol* 14: 81–93, 2014. doi:10.1038/nri3600.
22. **Iwasaki A, Medzhitov R.** Control of adaptive immunity by the innate immune system. *Nat Immunol* 16: 343–353, 2015. doi:10.1038/ni.3123.
23. **Ji JD, Park-Min KH, Ivashkiv LB.** Expression and function of semaphorin 3A and its receptors in human monocyte-derived macrophages. *Hum Immunol* 70: 211–217, 2009. doi:10.1016/j.humimm.2009.01.026.
24. **Kovach MA, Standiford TJ.** Toll like receptors in diseases of the lung. *Int Immunopharmacol* 11: 1399–1406, 2011. doi:10.1016/j.intimp.2011.05.013.
25. **Kumanogoh A, Kikutani H.** Immunological functions of the neuropilins and plexins as receptors for semaphorins. *Nat Rev Immunol* 13: 802–814, 2013. doi:10.1038/nri3545.
26. **Lantuéjoul S, Constantin B, Drabkin H, Brambilla C, Roche J, Brambilla E.** Expression of VEGF, semaphorin SEMA3F, and their common receptors neuropilins NP1 and NP2 in preinvasive bronchial lesions, lung tumours, and cell lines. *J Pathol* 200: 336–347, 2003. doi:10.1002/path.1367.
27. **Levy BD, Serhan CN.** Resolution of acute inflammation in the lung. *Annu Rev Physiol* 76: 467–492, 2014. doi:10.1146/annurev-physiol-021113-170408.
28. **Maus U, von Grote K, Kuziel WA, Mack M, Miller EJ, Cihak J, Stangassinger M, Maus R, Schlöndorff D, Seeger W, Lohmeyer J.** The role of CC chemokine receptor 2 in alveolar monocyte and neutrophil immigration in intact mice. *Am J Respir Crit Care Med* 166: 268–273, 2002. doi:10.1164/rccm.2112012.
29. **Maus UA, Waelsch K, Kuziel WA, Delbeck T, Mack M, Blackwell TS, Christman JW, Schlöndorff D, Seeger W, Lohmeyer J.** Monocytes are potent facilitators of alveolar neutrophil emigration during lung inflammation: role of the CCL2-CCR2 axis. *J Immunol* 170: 3273–3278, 2003. doi:10.4049/jimmunol.170.6.3273.
30. **Medford AR, Millar AB.** Vascular endothelial growth factor (VEGF) in acute lung injury (ALI) and acute respiratory distress syndrome (ARDS): paradox or paradigm? *Thorax* 61: 621–626, 2006. doi:10.1136/thx.2005.040204.
31. **Mendes-da-Cruz DA, Brignier AC, Asnafi V, Baleydier F, Messias CV, Lepelletier Y, Bedjaoui N, Renand A, Smaniotto S, Canioni D, Milpied P, Balabanian K, Bousso P, Leprêtre S, Bertrand Y, Dombret H, Ifrah N, Dardenne M, Macintyre E, Savino W, Hermine O.** Semaphorin 3F and neuropilin-2 control the migration of human T-cell precursors. *PLoS One* 9: e103405, 2014. doi:10.1371/journal.pone.0103405.
32. **Meyer N, Akdis CA.** Vascular endothelial growth factor as a key inducer of angiogenesis in the asthmatic airways. *Curr Allergy Asthma Rep* 13: 1–9, 2013. doi:10.1007/s11882-012-0317-9.
33. **Moran TP, Nakano H, Kondilis-Mangum HD, Wade PA, Cook DN.** Epigenetic control of Ccr7 expression in distinct lineages of lung dendritic cells. *J Immunol* 193: 4904–4913, 2014. doi:10.4049/jimmunol.1401104.
34. **Mucka P, Levonyak N, Geretti E, Zwaans BM, Li X, Adini I, Klagsbrun M, Adam RM, Bielenberg DR.** Inflammation and lymphedema are exacerbated and prolonged by neuropilin 2 deficiency. *Am J Pathol* 186: 2803–2812, 2016. doi:10.1016/j.ajpath.2016.07.022.
35. **Mühlenhoff M, Rollenhagen M, Werneburg S, Gerardy-Schahn R, Hildebrandt H.** Polysialic acid: versatile modification of NCAM, SynCAM 1 and neuropilin-2. *Neurochem Res* 38: 1134–1143, 2013. doi:10.1007/s11064-013-0979-2.
36. **Nakano H, Cook DN.** Pulmonary antigen presenting cells: isolation, purification, and culture. *Methods Mol Biol* 1032: 19–29, 2013. doi:10.1007/978-1-62703-496-8_2.
37. **Oussa NA, Dahmani A, Gomis M, Richaud M, Andreev E, Navab-Daneshmand AR, Taillefer J, Carli C, Boulet S, Sabbagh L, Labrecque N, Sapieha P, Delisle JS.** VEGF requires the receptor NRP-1 To inhibit lipopolysaccharide-dependent dendritic cell maturation. *J Immunol* 197: 3927–3935, 2016. doi:10.4049/jimmunol.1601116.
38. **Parker MW, Linkugel AD, Goel HL, Wu T, Mercurio AM, Vander Kooi CW.** Structural basis for VEGF-C binding to neuropilin-2 and sequestration by a soluble splice form. *Structure* 23: 677–687, 2015. doi:10.1016/j.str.2015.01.018.
39. **Prud'homme GJ, Glinka Y.** Neuropilins are multifunctional coreceptors involved in tumor initiation, growth, metastasis and immunity. *Oncotarget* 3: 921–939, 2012. doi:10.18632/oncotarget.626.
40. **Rossignol M, Gagnon ML, Klagsbrun M.** Genomic organization of human neuropilin-1 and neuropilin-2 genes: identification and distribution of splice variants and soluble isoforms. *Genomics* 70: 211–222, 2000. doi:10.1006/geno.2000.6381.
41. **Roy S, Bag AK, Singh RK, Talmadge JE, Batra SK, Datta K.** Multifaceted role of neuropilins in the immune system: potential targets for immunotherapy. *Front Immunol* 8: 1228, 2017. doi:10.3389/fimmu.2017.01228.
42. **Schellenburg S, Schulz A, Poitz DM, Muders MH.** Role of neuropilin-2 in the immune system. *Mol Immunol* 90: 239–244, 2017. doi:10.1016/j.molimm.2017.08.010.
43. **Shahraz A, Kopatz J, Mathy R, Kappler J, Winter D, Kapoor S, Schütza V, Scheper T, Gieselmann V, Neumann H.** Anti-inflammatory

activity of low molecular weight polysialic acid on human macrophages. *Sci Rep* 5: 16800, 2015. doi:10.1038/srep16800.

44. **Spence S, Greene MK, Fay F, Hams E, Saunders SP, Hamid U, Fitzgerald M, Beck J, Bains BK, Smyth P, Themistou E, Small DM, Schmid D, O'Kane CM, Fitzgerald DC, Abdelghany SM, Johnston JA, Fallon PG, Burrows JF, McAuley DF, Kissenpfennig A, Scott CJ.** Targeting Siglecs with a sialic acid-decorated nanoparticle abrogates inflammation. *Sci Transl Med* 7: 303ra140, 2015. doi:10.1126/scitranslmed.aab3459.
45. **Swendeman S, Mendelson K, Weskamp G, Horiuchi K, Deutsch U, Scherle P, Hooper A, Rafii S, Blobel CP.** VEGF-A stimulates ADAM17-dependent shedding of VEGFR2 and crosstalk between VEGFR2 and ERK signaling. *Circ Res* 103: 916–918, 2008. doi:10.1161/CIRCRESAHA.108.184416.
46. **Tang X, Sun J, Du L, Du H, Wang L, Mai J, Zhang F, Liu P.** Neuropilin-2 contributes to LPS-induced corneal inflammatory lymphangiogenesis. *Exp Eye Res* 143: 110–119, 2016. doi:10.1016/j.exer.2015.10.017.
47. **Werneburg S, Buettner FF, Erben L, Mathews M, Neumann H, Mühlenhoff M, Hildebrandt H.** Polysialylation and lipopolysaccharide-induced shedding of E-selectin ligand-1 and neuropilin-2 by microglia and THP-1 macrophages. *Glia* 64: 1314–1330, 2016. doi:10.1002/glia.23004.
48. **Wilson RH, Whitehead GS, Nakano H, Free ME, Kolls JK, Cook DN.** Allergic sensitization through the airway primes Th17-dependent neutrophilia and airway hyperresponsiveness. *Am J Respir Crit Care Med* 180: 720–730, 2009. doi:10.1164/rccm.200904-0573OC.
49. **Yuan L, Moyon D, Pardanaud L, Bréant C, Karkkainen MJ, Alitalo K, Eichmann A.** Abnormal lymphatic vessel development in neuropilin 2 mutant mice. *Development* 129: 4797–4806, 2002.
50. **Zhang P, Summer WR, Bagby GJ, Nelson S.** Innate immunity and pulmonary host defense. *Immunol Rev* 173: 39–51, 2000. doi:10.1034/j.1600-065X.2000.917306.x.
51. **Zhang X, Goncalves R, Mosser DM.** The isolation and characterization of murine macrophages. *Curr Protoc Immunol* Chapter 14: Unit 14.1, 2008. doi:10.1002/0471142735.im1401s83.
52. **Zuo L, Lucas K, Fortuna CA, Chuang CC, Best TM.** Molecular regulation of toll-like receptors in asthma and COPD. *Front Physiol* 6: 312, 2015. doi:10.3389/fphys.2015.00312.